Int. J. Solids Structures Vol. 30, No. 12, pp. 1679–1692, 1993
Printed in Great Britain

0020-7683/93 $6.00+ .00

A FINITE ELEMENT MODEL OF SINGLE-LAP ADHESIVE JOINTS

CHIEN-CHANG LIN and YEE-SHOWN LIN
Institute of Applied Mathematics, National Chung-Hsing University, Taichung, Taiwan, 40227, R.O.C.

(*Received* 25 *February* 1992; *in revised form* 2 *December* 1992)

Abstract—A finite element formulation for analysing the stresses in the adhesive of a single-lap joint is presented. The element is based on the Timoshenko beam theory and an assumed variation of the transverse shear stress and transverse normal stress through the thickness of the adherends. This element formulation in conjunction with the variational principle is used for determining constitutive relations in the adhesive layer. By means of the finite element formulation presented herein, any possible adhesive-layer conditions and nonidentical adherends in a single-lap joint are taken into account. Numerical examples are provided to illustrate the effects of the thickness of adhesive and nonidentical adherends on extreme stress in the adhesive.

1. INTRODUCTION

Most structures consist of an assembly of a number of individual elements connected to form a load transmission path. The use of adhesive joints is increasing because of a number of advantages they offer. In adhesive bonding, the aim is to transfer the load smoothly from one adherend to the other, minimizing the peak shear stresses and peel stresses in the adhesive layer.

Early theoretical studies of the stresses in adhesive joints were directed towards the single-lap joint. Goland and Reissner (1944) presented closed-form solutions of stress distribution in lap joints using a two-dimensional elasticity solution, and an assumption of relatively flexible adhesive layer. Later, this assumption for relatively flexible adhesive layers was formalized as the spring-beam analogy and used to study the stresses in a brazed tab fatigue specimen by Cornell (1953). Ojalvo and Eidinoff (1978) extended the theory of Goland and Reissner through the use of a more complete relation between shear strain and displacement corresponding to linearly varying displacements through the thickness of the adhesive. Roberts (1989) presented an analytical procedure based on beam theory solution and the assumption of relatively flexible adhesive layers.

Adams and Peppiatt (1974) and Adams and Wake (1984) used conventional finite elements to analyse the stress distribution in various lap joints. Rao *et al.* (1982) developed a 6-noded isoparametric interface element. Carpenter (1973, 1980) proposed an adhesive element based on the assumption common to the theories of Goland and Reissner as well as Ojalvo and Eidinoff. Further applications of interface elements to adhesive-bonded joint problems are investigated by some scholars. Previous methods for analysing single-lap adhesive joints were based on the assumption that the adhesive layer is relatively flexible. So, they can only deal with a certain range of flexibility of the adhesive layer but meet some difficulty for relatively inflexible adhesive layers. In adhesive bonding, loads are carried by the surface of the adherends in shear through a layer of adhesive. Therefore, shear effects are important in the adhesive-bonded joints. However, the foregoing references dealt with the beam theory without the effect of transverse shear.

The objective of this study is to develop a new finite element formulation for the adhesive that includes all transverse effects of the shear stress and normal stress in the adherend. Subsequently, its basic assumption involves the variation of the transverse shear stress and transverse normal stress through the thickness of the adherends. The element formulation in conjunction with the variational principle is used for determining the constitutive relations in the adhesive layer. By means of the finite element formulation presented

herein, any possible adhesive-layer conditions and nonidentical adherends with different thicknesses and different materials in a single-lap joint are taken into account.

2. FORMULATION

Considering a single-lap adhesive joint, the coordinate system geometry, and sign convention for shear and normal stress for an adhesive joint is shown in Fig. 1. For notational convenience, $(\ )^{(k)}$, $k = 1, 2$ will denote quantities associated with the kth adherend. We make the assumption that:

(1) Each adherend is considered to be in a state of plane stress.
(2) The longitudinal direct stresses in the adhesive are negligible when compared with those in the adherends.
(3) Longitudinal and transverse deflection in the bond material vary linearly through the adhesive thickness between the adherends.
(4) The shear stress in the adhesive is held constant through the thickness of the adhesive, and is equivalent to the mean stress.

The governing relations for the displacement vector $u^{(k)}$, $w^{(k)}$, the strain tensor $e_{ij}^{(k)}$ and the stress tensor $\sigma_{ij}^{(k)}$ in the kth adherend are expressed as follows:

(a) Stress–strain relations in the kth adherend

$$\sigma_{xx}^{(k)} = E^{(k)} e_{xx}^{(k)} + \nu^{(k)} \sigma_{zz}^{(k)}, \tag{1a}$$

$$\tau_{xz}^{(k)} = 2G^{(k)} e_{xz}^{(k)}, \tag{1b}$$

$$e_{zz}^{(k)} = -\nu^{(k)} e_{xx}^{(k)} + \left(\frac{1-\nu^2}{E}\right)^{(k)} \sigma_{zz}^{(k)}. \tag{1c}$$

(b) Strain–displacement relations in the kth adherend

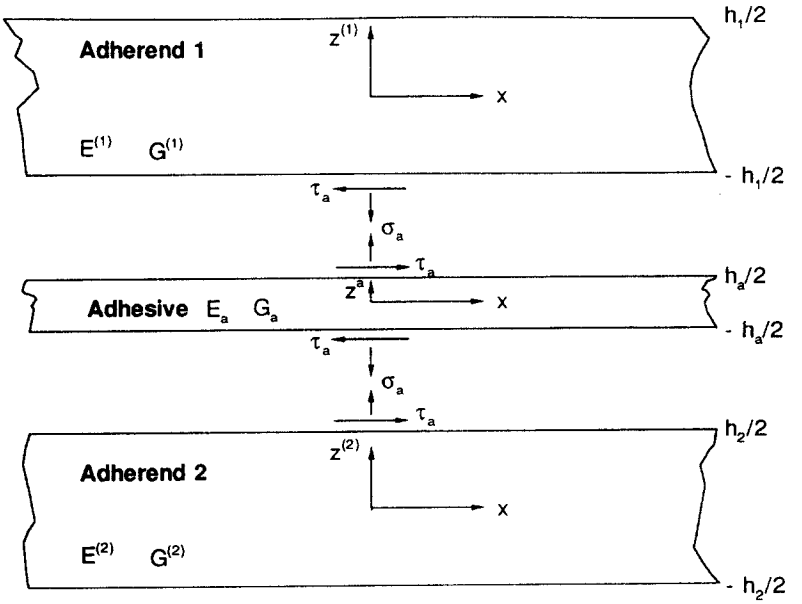

Fig. 1. Coordinates, geometry and sign conventions in adhesive joint.

$$e_{xx}^{(k)} = u_{,x}^{(k)}, \tag{2a}$$

$$e_{xz}^{(k)} = \tfrac{1}{2}(u_{,z}^{(k)} + w_{,x}^{(k)}), \tag{2b}$$

where $v^{(k)}$ is Poisson's ratio.

The following assumptions, the adhesive strain and the adhesive strain–stress relations, are given by:

(c) Strain–displacement relations in the adhesive

$$\gamma_a = \left[u^{(1)}\left(x, z^{(1)} = -\frac{h_1}{2}\right) - u^{(2)}\left(x, z^{(2)} = \frac{h_2}{2}\right)\right] \Big/ h_a, \tag{3a}$$

$$\varepsilon_a = \left[w^{(1)}\left(x, z^{(1)} = -\frac{h_1}{2}\right) - w^{(2)}\left(x, z^{(2)} = \frac{h_2}{2}\right)\right] \Big/ h_a. \tag{3b}$$

(d) Stress–strain relations in the adhesive

$$\tau_a = G_a \gamma_a, \tag{4a}$$

$$\sigma_a = E_a \varepsilon_a. \tag{4b}$$

The development of a constitutive relation for the adhesive is facilitated by using the variational principle for the boundary value problem of total quantities. The variational principle applied to the single-lap joint becomes

$$\int_0^L \left\{ \sum_{k=1}^{2} \int_{h_k/2}^{h_k/2} \left[\delta e_{xx}^{(k)} \sigma_{xx}^{(k)} + \delta e_{zz}^{(k)} \sigma_{zz}^{(k)} + 2\delta e_{xz}^{(k)} \tau_{xz}^{(\kappa)} + \delta \tau_{xz}^{(\kappa)} \left(u_{,z}^{(k)} + w_{,x}^{(k)} - \frac{\tau_{xz}^{(k)}}{G^{(k)}} \right) \right.\right.$$

$$\left. + \delta \sigma_{zz}^{(k)} \left(w_{,z}^{(k)} + v^{(k)} e_{xx}^{(k)} - \left(\frac{1-v^2}{E} \right)^{(k)} \sigma_{zz}^{(k)} \right) \right] \mathrm{d}z^{(k)} + \int_{-h_a/2}^{h_a/2} \left[\delta \gamma_a \tau_a + \delta \varepsilon_a \sigma_a \right.$$

$$\left.\left. + \delta \tau_a \left(\gamma_a - \frac{\tau_a}{G_a} \right) + \delta \sigma_a \left(\varepsilon_a - \frac{\sigma_a}{E_a} \right) \right] \mathrm{d}z^a \right\} \mathrm{d}x = \left[\sum_{k=1}^{2} \int_{-(h_k/2)}^{h_k/2} (\delta u^{(k)} t_x^{(k)} + \delta w^{(k)} t_z^{(k)}) \, \mathrm{d}z^{(k)} \right]_0^L, \tag{5}$$

where $t_x^{(k)}$, $t_z^{(k)}$ are the boundary tractions.

Based on Timoshenko beam theory, the trial displacement field of the adherends is given by

$$u^{(1)}(x, z^{(1)}) = U^{(1)}(x) + z^{(1)} \theta^{(1)}(x), \tag{6a}$$

$$u^{(2)}(x, z^{(2)}) = U^{(2)}(x) + z^{(2)} \theta^{(2)}(x), \tag{6b}$$

$$w^{(1)}(x, z^{(1)}) = W^{(1)}(x), \tag{6c}$$

$$w^{(2)}(x, z^{(2)}) = W^{(2)}(x), \tag{6d}$$

where $U^{(k)}$, $\theta^{(k)}$, $W^{(k)}$ are mid-plane displacements in the kth adherend.

The transverse shear stress and normal stress field distribution through the thickness of the kth adherend are taken to be

$$\tau_{xz}^{(1)} = \frac{3Q^{(1)}}{2h_1} \left[1 - \left(\frac{2z^{(1)}}{h_1} \right)^2 \right] + \tau_a \left[3 \left(\frac{z^{(1)}}{h_1} \right)^2 - \frac{z^{(1)}}{h_1} - \frac{1}{4} \right], \tag{7a}$$

$$\sigma_{zz}^{(1)} = \frac{\sigma_a}{2} \left[1 - \frac{3z^{(1)}}{h_1} + 4 \left(\frac{z^{(1)}}{h_1} \right)^3 \right] \quad \text{for} \quad -\frac{h_1}{2} \leqslant z^{(1)} \leqslant \frac{h_1}{2}, \tag{7b}$$

and

$$\tau_{xz}^{(2)} = \frac{2Q^{(2)}}{2h_2}\left[1-\left(\frac{2z^{(2)}}{h_2}\right)^2\right]+\tau_a\left[3\left(\frac{z^{(2)}}{h_2}\right)^2+\frac{z^{(2)}}{h_2}-\frac{1}{4}\right], \tag{7c}$$

$$\sigma_{zz}^{(2)} = \frac{\sigma_a}{2}\left[1+\frac{3z^{(2)}}{h_2}-4\left(\frac{z^{(2)}}{h_2}\right)^3\right] \quad \text{for} \quad -\frac{h_2}{2} \leqslant z^{(2)} \leqslant \frac{h_2}{2}, \tag{7d}$$

where

$$Q^{(k)} = \int_{-(h_k/2)}^{h_k/2} \tau_{xz}^{(k)}\, \mathrm{d}z^{(k)}. \tag{7e}$$

Let us consider an infinitesimal element of the adherend which is supported at its ends, as illustrated in Fig. 2. Assuming that the load and intensity σ_a are uniformly distributed, we can obtain the transverse normal stress field $\sigma_{zz}^{(k)}$ by using the Airy function. The transverse shear stresses field $\tau_{xz}^{(k)}$ may be represented by quadratic polynomials of $z^{(k)}$. Their coefficients are computed by using eqns (7e) and boundary condition equations (8a–d):

$$\tau_{xz}^{(1)}\left(x, z^{(1)} = \frac{h_1}{2}\right) = 0, \tag{8a}$$

$$\tau_{xz}^{(1)}\left(x, z^{(1)} = -\frac{h_1}{2}\right) = \tau_a, \tag{8b}$$

$$\tau_{xz}^{(2)}\left(x, z^{(2)} = \frac{h_2}{2}\right) = \tau_a, \tag{8c}$$

$$\tau_{xz}^{(2)}\left(x, z^{(2)} = -\frac{h_2}{2}\right) = 0. \tag{8d}$$

Substituting eqns (2), (3), (4), (6) and (7) into eqn (5) and using Gauss's theorem, one obtains the following equilibrium equations, boundary conditions and constitutive equations which automatically include the appropriate shear correction factors.

Equilibrium equations

$$N_{,x}^{(1)} - \tau_a = 0, \tag{9a}$$

$$N_{,x}^{(2)} + \tau_a = 0, \tag{9b}$$

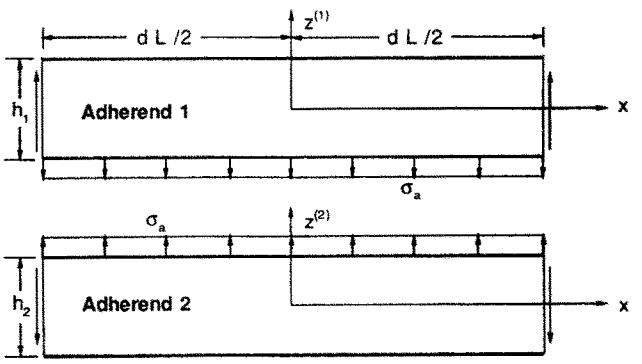

Fig. 2. Infinitesimal adherend element.

$$M_{,x}^{(1)} - Q^{(1)} + \frac{h_1}{2}\tau_a = 0, \tag{9c}$$

$$M_{,x}^{(2)} - Q^{(2)} + \frac{h_2}{2}\tau_a = 0, \tag{9d}$$

$$Q_{,x}^{(1)} - \sigma_a = 0, \tag{9e}$$

$$Q_{,x}^{(2)} + \sigma_a = 0, \tag{9f}$$

where stress force resultants are defined by

$$N^{(k)} = \int_{-(h_k/2)}^{h_k/2} \sigma_{xx}^{(k)}\, \mathrm{d}z^{(k)}, \tag{9g}$$

$$M^{(k)} = \int_{-(h_k/2)}^{h_k/2} \sigma_{xx}^{(k)} z^{(k)}\, \mathrm{d}z^{(k)}. \tag{9h}$$

Boundary conditions

The boundary condition at $x = 0$ and L:

$$\delta U^{(k)} = 0 \quad \text{or} \quad T_x^{(k)} = N^{(k)}, \tag{10a}$$

$$\delta\theta^{(k)} = 0 \quad \text{or} \quad T_M^{(k)} = M^{(k)}, \tag{10b}$$

$$\delta W^{(k)} = 0 \quad \text{or} \quad T_z^{(k)} = Q^{(k)}, \quad k = 1, 2, \tag{10c}$$

where

$$T_x^{(k)} = \int_{-(h_k/2)}^{h_k/2} t_x^{(k)}\, \mathrm{d}z^{(k)}, \tag{10d}$$

$$T_M^{(k)} = \int_{-(h_k/2)}^{h_k/2} z^{(k)} t_x^{(k)}\, \mathrm{d}z^{(k)}, \tag{10e}$$

$$T_z^{(k)} = \int_{-(h_k/2)}^{h_k/2} t_z^{(k)}\, \mathrm{d}z^{(k)}. \tag{10f}$$

Constitutive equations

$$Q^{(1)} = \left(\frac{5G^{(1)}h_1}{6} + \frac{h_1^2 R}{144}\right)(\theta^{(1)} + W_{,x}^{(1)}) + \frac{h_1 h_2 R}{144}(\theta^{(2)} + W_{,x}^{(2)}) + \frac{h_1 R}{12}\left(U^{(1)} - U^{(2)} - \frac{h_1}{2}\theta^{(1)} - \frac{h_2}{2}\theta^{(2)}\right), \tag{11a}$$

$$Q^{(2)} = \frac{h_1 h_2 R}{144}(\theta^{(1)} + W_{,x}^{(1)}) + \left(\frac{5G^{(2)}h_2}{6} + \frac{h_2^2 R}{144}\right)(\theta^{(2)} + W_{,x}^{(2)}) + \frac{h_2 R}{12}\left(U^{(1)} - U^{(2)} - \frac{h_1}{2}\theta^{(1)} - \frac{h_2}{2}\theta^{(2)}\right), \tag{11b}$$

$$\tau_a = \frac{h_1 R}{12}(\theta^{(1)} + W_{,x}^{(1)}) + \frac{h_2 R}{12}(\theta^{(2)} + W_{,x}^{(2)}) + R\left(U^{(1)} - U^{(2)} - \frac{h_1}{2}\theta^{(1)} - \frac{h_2}{2}\theta^{(2)}\right), \tag{11c}$$

$$\sigma_a = P(W^{(1)} - W^{(2)}) + h_1 v^{(1)} P\left(\frac{1}{2} U_{,x}^{(1)} - \frac{h_1}{10}\theta_{,x}^{(1)}\right) + h_2 v^{(2)} P\left(\frac{1}{2} U_{,x}^{(2)} + \frac{h_2}{10}\theta_{,x}^{(2)}\right), \quad (11d)$$

where correction factors are

$$R = 1\Big/\left(\frac{h_1}{8G^{(1)}} + \frac{h_2}{8G^{(2)}} + \frac{h_a}{G_a}\right), \quad (12a)$$

$$P = 1\Big/\left[\frac{13h_1}{35}\left(\frac{1-v^2}{E}\right)^{(1)} + \frac{13h_2}{35}\left(\frac{1-v^2}{E}\right)^{(2)} + \frac{h_a}{E_a}\right]. \quad (12b)$$

The remaining constitutive equations for $N^{(k)}$, $M^{(k)}$ are obtained by substituting eqns (1a), (7b), (7d), (11d) into eqns (9g), (9h):

$$N^{(1)} = \left(E^{(1)}h_1 + \frac{(v^{(1)})^2 h_1^2 P}{4}\right) U_{,x}^{(1)} - \frac{(v^{(1)})^2 h_1^3 P}{20}\theta_{,x}^{(1)} + \frac{v^{(1)}v^{(2)}h_1 h_2 P}{4} U_{,x}^{(2)} + \frac{v^{(1)}v^{(2)}h_1 h_2^2 P}{20}\theta_{,x}^{(2)} + \frac{v^{(1)}h_1 P}{2}(W^{(1)} - W^{(2)}), \quad (13a)$$

$$N^{(2)} = \frac{v^{(1)}v^{(2)}h_1 h_2 P}{4} U_{,x}^{(1)} - \frac{v^{(1)}v^{(2)}h_1^2 h_2 P}{20}\theta_{,x}^{(1)} + \left(E^{(2)}h_2 + \frac{(v^{(2)})^2 h_2^2 P}{4}\right) U_{,x}^{(2)} + \frac{(v^{(2)})^2 h_2^3 P}{20}\theta_{,x}^{(2)} + \frac{v^{(2)}h_2 P}{2}(W^{(1)} - W^{(2)}), \quad (13b)$$

$$M^{(1)} = -\frac{(v^{(1)})^2 h_1^3 P}{20} U_{,x}^{(1)} + \left(\frac{E^{(1)}h_1^3}{12} + \frac{(v^{(1)})^2 h_1^4 P}{100}\right)\theta_{,x}^{(1)} - \frac{v^{(1)}v^{(2)}h_1^2 h_2 P}{20} U_{,x}^{(2)} - \frac{v^{(1)}v^{(2)}h_1^2 h_2^2 P}{100}\theta_{,x}^{(2)} - \frac{v^{(1)}h_1^2 P}{10}(W^{(1)} - W^{(2)}), \quad (13c)$$

$$M^{(2)} = \frac{v^{(1)}v^{(2)}h_1 h_2^2 P}{20} U_{,x}^{(1)} - \frac{v^{(1)}v^{(2)}h_1^2 h_2^2 P}{100}\theta_{,x}^{(1)} + \frac{(v^{(2)})^2 h_2^3 P}{20} U_{,x}^{(2)} + \left(\frac{E^{(2)}h_2^3}{12} + \frac{(v^{(2)})^2 h_2^4 P}{100}\right)\theta_{,x}^{(2)} + \frac{v^{(2)}h_2^2 P}{10}(W^{(1)} - W^{(2)}). \quad (13d)$$

3. FINITE ELEMENT FORMULATION

The principle of virtual work applied to a single-lap adhesive joint becomes

$$\int_0^L \delta\{\varepsilon\}^{\mathrm{T}}\{\sigma\}\,\mathrm{d}x = \delta\{u\}^{\mathrm{T}}\{q\}, \quad (14)$$

where

$$\{\varepsilon\}^{\mathrm{T}} = [U_{,x}^{(1)} \quad \theta_{,x}^{(1)} \quad \theta^{(1)} + W_{,x}^{(1)} \quad U^{(1)} - U^{(2)} - \frac{h_1}{2}\theta^{(1)} - \frac{h_2}{2}\theta^{(2)} \quad W^{(1)} - W^{(2)} \quad U_{,x}^{(2)} \quad \theta_{,x}^{(2)} \quad \theta^{(2)} + W_{,x}^{(2)}], \quad (15a)$$

$$\{\sigma\}^{\mathrm{T}} = [N^{(1)} \quad M^{(1)} \quad Q^{(1)} \quad \tau_a \quad \sigma_a \quad N^{(2)} \quad M^{(2)} \quad Q^{(2)}], \quad (15b)$$

$$\{u\}^{\mathrm{T}} = [U^{(1)} \quad \theta^{(1)} \quad W^{(1)} \quad U^{(2)} \quad \theta^{(2)} \quad W^{(2)}], \quad (15c)$$

$$\{q\}^{\mathrm{T}} = [N^{(1)} \quad M^{(1)} \quad Q^{(1)} \quad N^{(2)} \quad M^{(2)} \quad Q^{(2)}]. \quad (15d)$$

Let the domain L be subdivided into a finite number N_1 of individual finite elements L_e, $e = 1, 2, \ldots, N_1$. A single-lap joint element with nodes offset against both the upper and lower adherend is developed. The schematic of the element is shown in Fig. 3. For each element the generalized displacement $\tilde{u}^{(k)}$ in the kth adherend is interpolated by the nodal displacement $\tilde{U}_i$ at node i in the element:

$$\tilde{u}^{(1)} = \sum_{i=1}^{N_n} N_i(\xi)\tilde{U}_{2i-1}, \tag{16a}$$

$$\tilde{u}^{(2)} = \sum_{i=1}^{N_n} N_i(\xi)\tilde{U}_{2i}, \tag{16b}$$

where $2N_n$ is the number of nodes of the element, $N_i(\xi)$ is the isoparametric interpolation function and

$$\tilde{U}_i = \begin{bmatrix} U_i \\ \theta_i \\ W_i \end{bmatrix}, \quad i = 1, 2, \ldots, 2N_n. \tag{17}$$

It is now straightforward to define matrix $[B]$ according to

$$\{\varepsilon\} = [B]\{U\}, \tag{18}$$

where

$$\{U\}^{\mathrm{T}} = [\tilde{U}_1^{\mathrm{T}} \quad \tilde{U}_2^{\mathrm{T}} \quad \ldots \quad U_{2N_n}^{\mathrm{T}}], \tag{19a}$$

$$[B] = [B_1 \quad B_2 \quad \ldots \quad B_{N_n}], \tag{19b}$$

$$B_i = \begin{bmatrix} \dfrac{\partial N_i}{\partial x} & 0 & 0 & 0 & 0 & 0 \\ 0 & \dfrac{\partial N_i}{\partial x} & 0 & 0 & 0 & 0 \\ 0 & N_i & \dfrac{\partial N_i}{\partial x} & 0 & 0 & 0 \\ N_i & -\dfrac{h_1}{2}N_i & 0 & -N_i & -\dfrac{h_2}{2}N_i & 0 \\ 0 & 0 & N_i & 0 & 0 & -N_i \\ 0 & 0 & 0 & \dfrac{\partial N_i}{\partial x} & 0 & 0 \\ 0 & 0 & 0 & 0 & \dfrac{\partial N_i}{\partial x} & 0 \\ 0 & 0 & 0 & 0 & N_i & \dfrac{\partial N_i}{\partial x} \end{bmatrix}, \quad i = 1 \sim N_n, \tag{19c}$$

the constitutive equations (11) and (13) can be expressed in the form

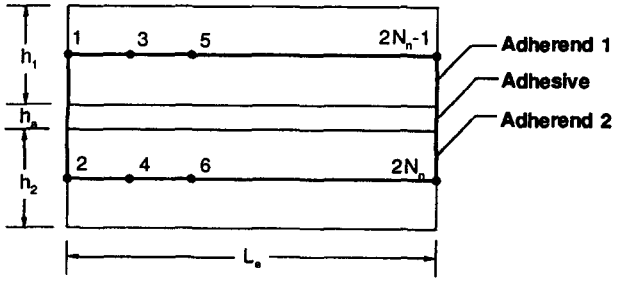

Fig. 3. Schematic of element.

$$\{\sigma\} = [D^e]\{\varepsilon\}, \tag{20}$$

where $[D^e]$ is an 8×8 modulus matrix:

$$[D^e] = \begin{bmatrix} D_1 & 0 & D_5 & 0 \\ 0 & D_2 & 0 & D_6 \\ D_5^T & 0 & D_3 & 0 \\ 0 & D_6^T & 0 & D_4 \end{bmatrix}, \tag{21}$$

$$D_1 = \begin{bmatrix} E^{(1)}h_1 + \dfrac{(v^{(1)})^2 h_1^2 P}{4} & -\dfrac{(v^{(1)})^2 h_1^3 P}{20} \\ -\dfrac{(v^{(1)})^2 h_1^3 P}{20} & \dfrac{E^{(1)}h_1^3}{12} + \dfrac{(v^{(1)})^2 h_1^4 P}{100} \end{bmatrix}, \tag{22a}$$

$$D_2 = \begin{bmatrix} \dfrac{5G^{(1)}h_1}{6} + \dfrac{h_1^2 R}{144} & \dfrac{h_1 R}{12} \\ \dfrac{h_1 R}{12} & R \end{bmatrix}, \tag{22b}$$

$$D_3 = \begin{bmatrix} P & \dfrac{v^{(2)}h_2 P}{2} & \dfrac{v^{(2)}h_2^2 P}{10} \\ \dfrac{v^{(2)}h_2 P}{2} & E^{(2)}h_2 + \dfrac{(v^{(2)})^2 h_2^2 P}{4} & \dfrac{(v^{(2)})^2 h_2^3 P}{20} \\ \dfrac{v^{(2)}h_2^2 P}{10} & \dfrac{(v^{(2)})^2 h_2^3 P}{20} & \dfrac{E^{(2)}h_2^3}{12} + \dfrac{(v^{(2)})^2 h_2^4 P}{100} \end{bmatrix}, \tag{22c}$$

$$D_4 = \left[\frac{5G^{(2)}h_2}{6} + \frac{h_2^2 R}{144}\right], \tag{22d}$$

$$D_5 = \begin{bmatrix} \dfrac{v^{(1)}h_1 P}{2} & \dfrac{v^{(1)}v^{(2)}h_1 h_2 P}{4} & \dfrac{v^{(1)}v^{(2)}h_1 h_2^2 P}{20} \\ -\dfrac{v^{(1)}h_1^2 P}{10} & -\dfrac{v^{(1)}v^{(2)}h_1^2 h_2 P}{20} & -\dfrac{v^{(1)}v^{(2)}h_1^2 h_2^2 P}{100} \end{bmatrix}, \tag{22e}$$

$$D_6 = \begin{bmatrix} \dfrac{h_1 h_2 R}{144} \\ \dfrac{h_2 R}{12} \end{bmatrix}. \tag{22f}$$

The element stiffness matrix $[K^e]$ of the single-lap joints is obtained as

$$[K^e] = \int_0^{L_e} [B]^T [D^e][B]\, dx. \tag{23}$$

4. NUMERICAL RESULTS

Example 1

The first demonstration example is the analysis of a single-lap joint subject to axial force p and bending $M = p(h_1 + h_2)/2$, as shown in Fig. 4, having the following properties: length of joint $L = 12.7$ mm; adherend thickness $h_1 = h_2 = 1.0$ mm; adhesive thickness

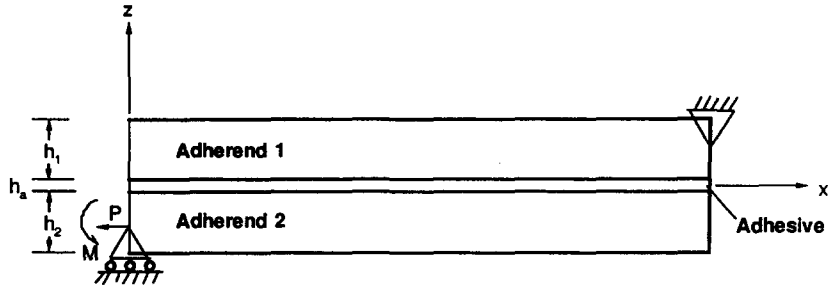

Fig. 4. Single-lap joint and idealization.

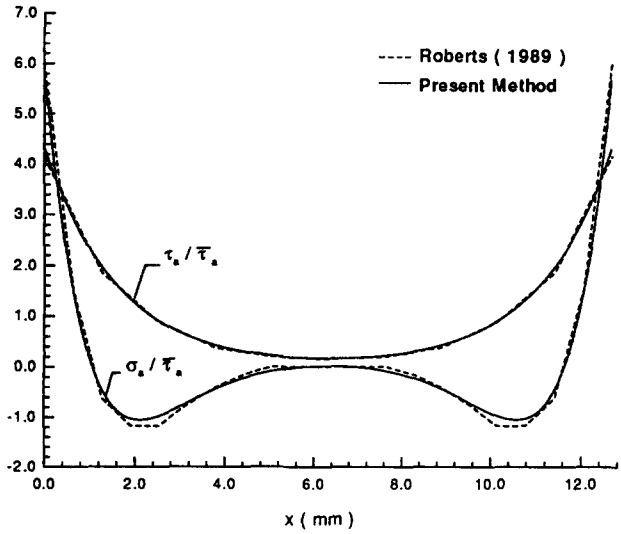

Fig. 5. Results for single lap joint—comparison with Roberts' results.

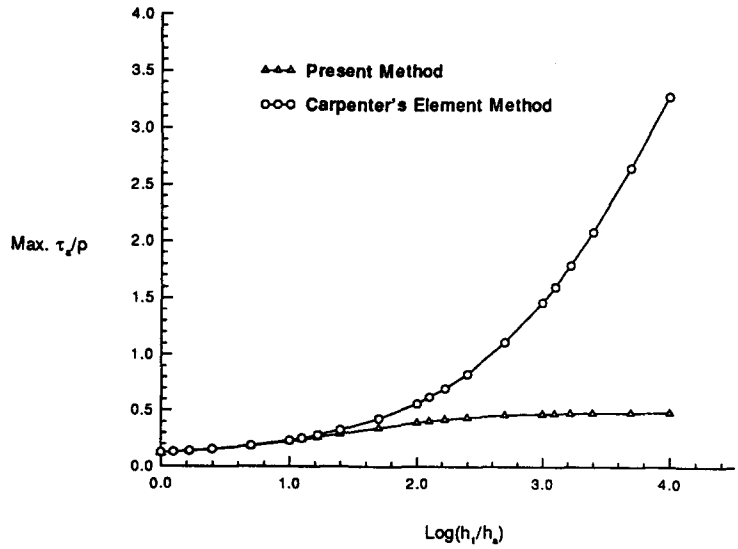

Fig. 6. Maximum shear stress in the adhesive for different h_a—comparison with Carpenter's element analysis results.

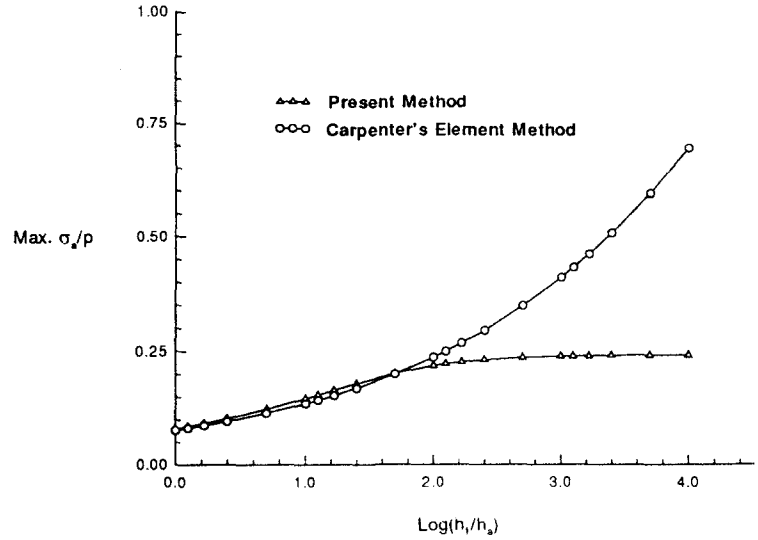

Fig. 7. Maximum normal stress in the adhesive for different h_a—comparison with Carpenter's element analysis results.

$h_a = 0.4$ mm; Young's modulus of adherend $E^{(1)} = E^{(2)} = 80{,}000$ N mm^{-2}; Poisson's ratio $\nu^{(1)} = \nu^{(2)} = 0.3$; Young's modulus of adhesive $E_a = 2000$ N mm^{-2} and shear modulus of adhesive $G_a = 800$ N mm^{-2}, the results are presented in nondimensional form in Fig. 5, in which $\bar{\tau}_a$ is the average shear force per unit length in the adhesive. The present results are in good agreement with previously analytical results obtained by Roberts (1989).

Example 2

The second example deals with the analysis of a single-lap joint subject to axial force p. This example illustrates the effect of the thickness of the adhesive layer on the shear and normal stress in the adhesive layer, with the following properties: length of joint $L = 10$ mm; adherend thickness $h_1 = h_2 = 1$ mm; $E^{(1)} = E^{(2)} = 80{,}000$ N mm^{-2}; $\nu^{(1)} = \nu^{(2)} = 0.3$; $E_a = 2000$ N mm^{-2}; $G_a = 800$ N mm^{-2} and adhesive thickness h_a is variable from 1 mm to 0.0001 mm. Figures 6 and 7 show comparison between the present results and results

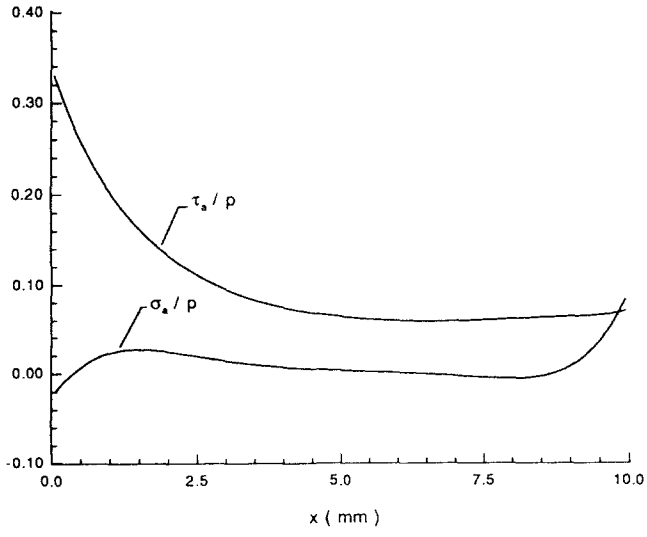

Fig. 8. Shear and normal stress in the adhesive for $h_1 = h_2$, $E^{(1)}/E^{(2)} = 10$.

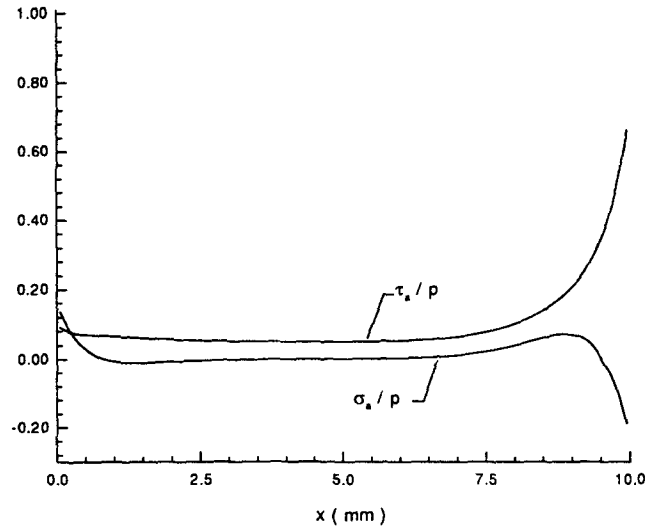

Fig. 9. Shear and normal stress in the adhesive for $h_1 = h_2$, $E^{(1)}/E^{(2)} = 0.1$.

using Carpenter's finite element analysis for determining the maximum shear stress and normal stress in the adhesive. It is easily seen that Carpenter's finite element analysis results are inadequate for convergence when the thickness of the adhesive layer in a joint is extremely small compared with that of the adherend. Carpenter's finite element formulation is based on the assumption common to the theories of Goland and Reissner as well as Ojalvo and Eidinoff. Equations (24) show the stress–displacement relations in the adhesive layer. The singularity occurs when the adhesive thickness h_a approaches zero:

$$\tau_a = \frac{g_a}{h_a}\left[(U^{(1)} - U^{(2)}) + \alpha_1 h_a\left(\frac{W^{(1)'} + W^{(2)'}}{2}\right) + \alpha_3 z^a (W^{(1)'} - W^{(2)'})\right], \tag{24a}$$

$$\sigma_a = \frac{E_a}{h_a}(W^{(1)} - W^{(2)}). \tag{24b}$$

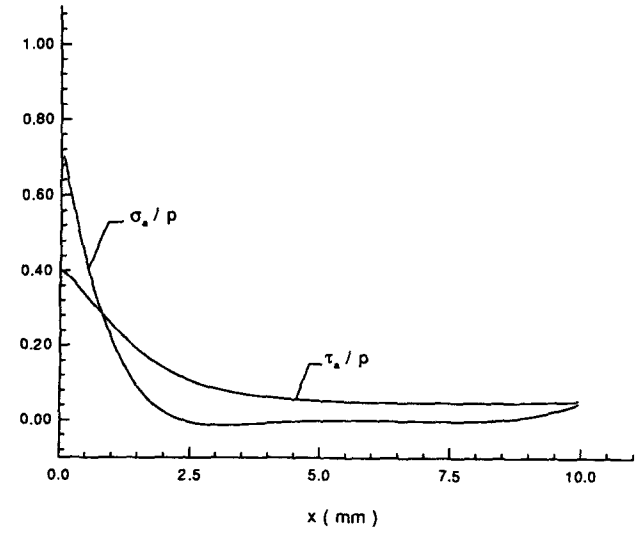

Fig. 10. Shear and normal stress in the adhesive for $E^{(1)} = E^{(2)}$, $h_1/h_2 = 10$.

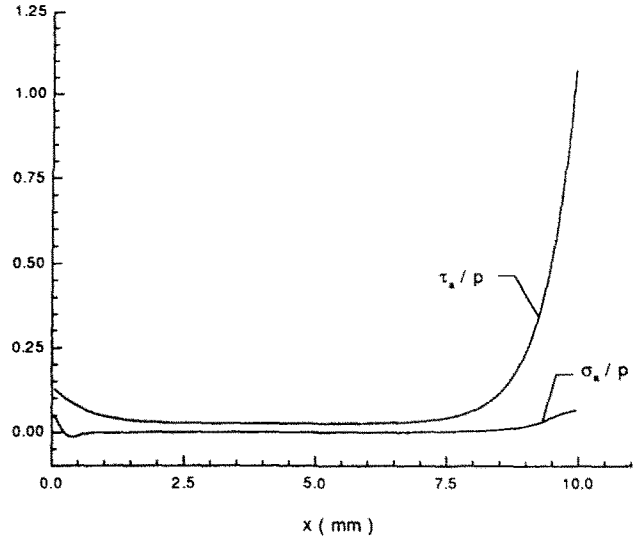

Fig. 11. Shear and normal stress in the adhesive for $E^{(1)} = E^{(2)}$, $h_1/h_2 = 0.1$.

Example 3

The third example is similar to the second example, which illustrates the effect of the material properties and the thickness of two adherends on the maximum shear and maximum normal stress in the adhesive; the parameters are $L = 10$ mm; $h_2 = 1$ mm; $E^{(2)} = 80{,}000$ N mm^{-2}; $h_a = 0.4$ mm; $E_a = 2000$ N mm^{-2}; $G_a = 800$ N mm^{-2}; $\nu^{(1)} = \nu^{(2)} = 0.3$; $E^{(1)}/E^{(2)} = 0.1$–10; $h_1/h_2 = 0.1$–10. Figures 8–11 show the distributions of shear and normal stresses in the adhesive with different adherend thickness and different adherend materials. Figures 12–15 show the extreme shear and normal stresses in the adhesive acting on both ends of the joint. These results reveal that the maximum shear and normal stress always occur at different end zones of the joint and depend greatly on the ratio of $E^{(1)}/E^{(2)}$ and h_1/h_2.

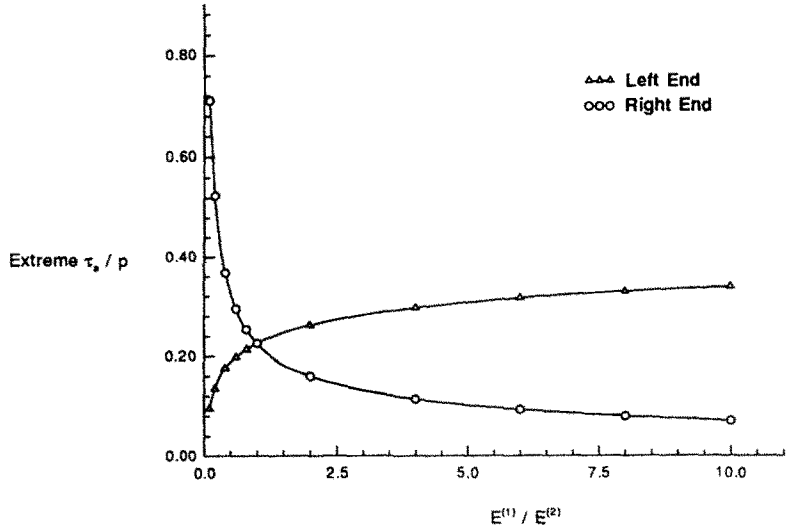

Fig. 12. Extreme shear stress in the adhesive at both ends for $h_1 = h_2$ via different $E^{(1)}/E^{(2)}$.

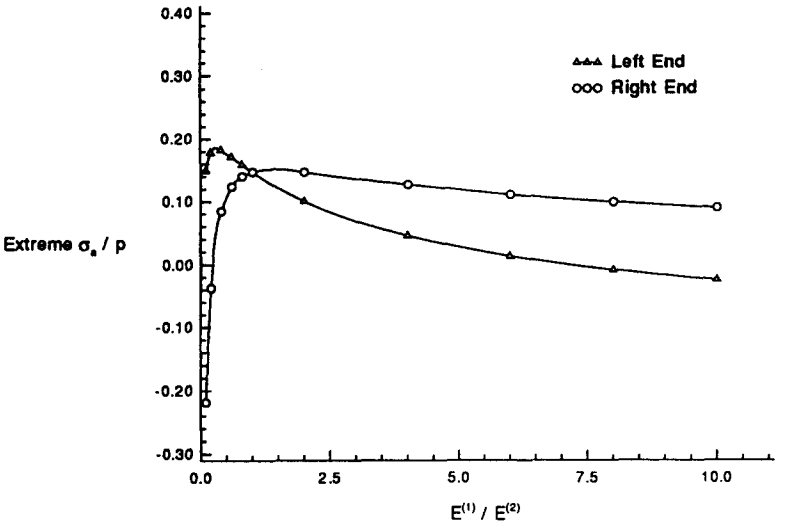

Fig. 13. Extreme normal stress in the adhesive at both ends for $h_1 = h_2$ via different $E^{(1)}/E^{(2)}$.

5. CONCLUSION

A finite element formulation for single-lap adhesive joints is presented which can analyse the distribution of the shear and normal stresses in a variety of adhesive joints with any possible adhesive-layer conditions and nonidentical adherends. The results obtained are in good agreement with the previously obtained analytical results for a relatively flexible adhesive layer in the joint. The results also reveal that the maximum shear and normal stresses are found to increase as the thickness of the adhesive thins. The variation $E^{(1)}$ and $E^{(2)}$ or h_1 and h_2 might have a significant effect on the magnitudes of the maximum shear and normal stresses, which always occur at different end zones, in the adhesive layer of the joint. Thus, the present model provides a rapid and realistic assessment of the stresses in single-lap adhesive joints for use in designing or repairing a joint.

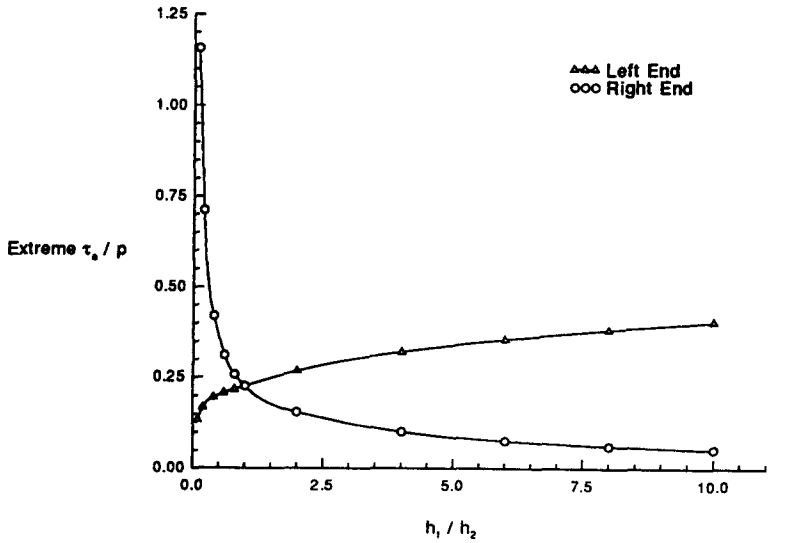

Fig. 14. Extreme shear stress in the adhesive at both ends for $E^{(1)} = E^{(2)}$ via different h_1/h_2.

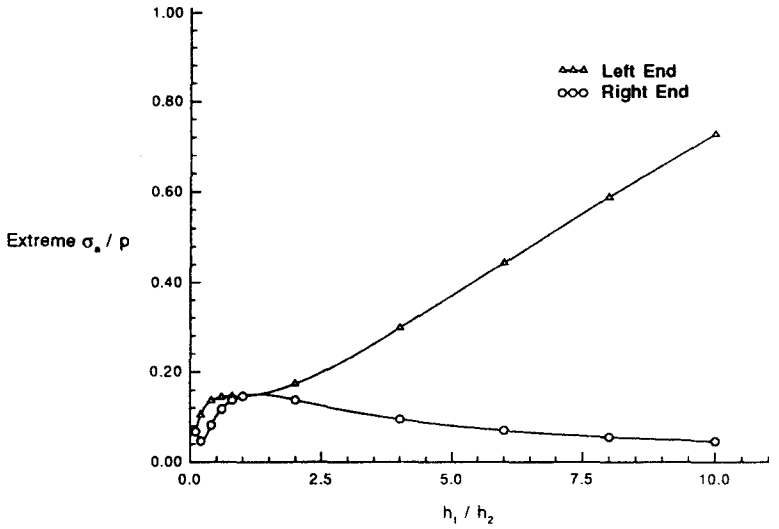

Fig. 15. Extreme normal stress in the adhesive at both ends for $E^{(1)} = E^{(2)}$ via different h_1/h_2.

REFERENCES

Adams, R. D. and Peppiatt, N. A. (1974). Stress analysis of adhesive bonded lap joints. *J. Strain Anal.* **9**(3), 185–196.

Adams, R. D. and Wake, W. C. (1984). *Structural Adhesive Joints in Engineering*. Elsevier, London.

Carpenter, W. C. (1973). Finite element analysis of bonded connections. *Int. J. Numer. Meth. Engng* **6**, 450–451.

Carpenter, W. C. (1980). Stresses in bonded connection using finite elements. *Int. J. Num. Meth. Engng* **15**, 1659–1680.

Cornell, R. W. (1953). Determination of stresses in cemented lamp joints. *J. Appl. Mech.* **20**, 355–364.

Goland, M. and Reissner, E. (1944). The stresses in cemented joints. *J. Appl. Mech.* **11**, A17–A22.

Ojalvo, I. U. and Eidinoff, H. L. (1978). Bond thickness effects upon stresses in single-lap adhesive joints. *AIAA Jl* **16**(3), 204–211.

Rao, B. N., Rao, Y. V. K. S. and Yadagiri, S. (1982). Analysis of composite bonded joints. *Fibre Science and Technology* **17**, 77–90.

Roberts, T. M. (1989). Shear and normal stresses in adhesive joints. *J. Engng Mech. Div. ASCE* **115**(11), 2460–2479.